Check for
updates

Routing a quantum state in a bio-inspired network

Elham Faraji[1,2,3,4] **· Alireza Nourmandipour**[5] **· Stefano Mancini**[2,4] **·**
Marco Pettini[3,6] **· Roberto Franzosi**[4,7,8]

Abstract
We consider a spin network resembling an α-helix structure and study quantum information transfer over this bio-inspired network. The model we use is the Davydov model in its elementary version without a phononic environment. We investigate analytically and numerically the perfect state transfer (PST) in such a network which provides an upper bound on the probability of quantum states transfer from one node to another. We study PST for different boundary conditions on the network and show it is reachable between certain nodes and with suitable spin–spin couplings.

Keywords Spin network · Perfect state transfer · Bio-inspired structure

1 Introduction

In extensive networking quantum information processing, reliable communication represents one of the most prominent challenges to overcome [1]. From this perspective, the problem of high-fidelity quantum state/information transfer and quantum network engineering have been largely studied either theoretically [2] or experimentally [3].

✉ Elham Faraji
  e.faraji@fz-juelich.de

1   Computational Biomedicine, Institute for Advanced Simulation IAS-5, and Institute of
    Neuroscience and Medicine INM-9, Forschungszentrum Jülich, 52428 Jülich, Germany

2   School of Science and Technology, University of Camerino, 62032 Camerino, Italy

3   Aix Marseille Univ, Université de Toulon, CNRS, CPT, Marseille, France

4   INFN Sezione di Perugia, 06123 Perugia, Italy

5   Department of Physics, Sirjan University of Technology, Sirjan 7813733385, Iran

6   CNRS Centre de Physique Théorique UMR7332, 13288 Marseille, France

7   DSFTA, University of Siena, Via Roma 56, 53100 Siena, Italy

8   QSTAR and INO-CNR, Largo Enrico Fermi 2, 50125 Florence, Italy

---

 Springer

In addition to being an essential building block for the progress of quantum information technologies applications [4–6], such as quantum cryptography, quantum computation and teleportation, the investigation of optimal state transfer represents also a valuable tool for the investigation of the fundamental physics [7, 8]. A network of spins [9] interacting by an appropriate Hamiltonian, such as the XY or the Heisenberg one [10], is a paradigm for the realization of long-distance communication devices. Here, the information encoded in the excitations of the network of spins can be shared between the parties, provided that one has quantum state transfer with high fidelity. In these cases, quantum information high-fidelity transfer origins from suitable quantum interference effects induced from the network dynamics [11].

Nowadays, experimentalists are faced with the problem of synthesizing spin networks reliable to perform high-performance state transfer. For instance, in a possible scheme, qubits should be stored in quantum chips whose dimensions are comparable to one of the classical devices, and which are confined into hosting-equipments, at near absolute-zero temperature, to maintain quantum coherence. Furthermore, the engineering of a chain of qubits is challenging. A possible setup considers trapping the (two-level) atoms in a cavity. In this case, an external classical field confines the atoms in the minima of a profound optical-lattice potential, whereas the atoms interact via cavity-induced atom-atom interactions [12].

Recent advances in quantum science have pioneered the way towards the description of biological realm phenomena in the framework of quantum mechanics. Indeed, quantum mechanics suitably describes properties of systems at nanoscale or lower, and many life processes, such as photosynthesis, vision, and respiration [13], take place at these scales. For instance, it has been proposed that the nuclear spins of phosphorus atoms could act as qubits in the brain which would enable it to function like a quantum computer [14]. Also, new evidences suggest that quantum effects help plants to turn sunlight into fuel [15]. There are strong witnesses that the migratory birds have a sort of quantum compass which helps them to exploit the earth's magnetic fields for navigation [16]. Furthermore, examining the quantum mechanics' role in the matter and energy of living microorganisms could pave the way for our understanding of the origin of life.

Remarkably, most processes in which the quantum nature emerges involve energy transfer to the living matter. Furthermore, there are considerable shreds of evidence that, the light-initiated reactions in living organisms, even at ambient conditions, display quantum coherent behavior [17]. In the simplest scenario, enhancement in electron transport is driven by quantum coherent processes where electronic excitations with a well-defined phase relationship at the molecular scale take place. In this regard, there are no better candidates than electrons for energy transfer, to understand the relevant quantum effects in living matter. Many works have been devoted to studying energy and information transmission efficiency in living organizations, such as in photosynthetic processes, in the framework of the quantum information processing [18–20]. Several possible theoretical frameworks have been proposed to understand the nature of exciton propagation on a lattice [21, 22], where the electron distribution belongs to this class of phenomena. In a seminal work, Davydov proposed that the mechanism for energy storage and transport in biomolecules could be considered soliton formation and propagation. In this scenario, the self-localization of quantum units of peptide

vibrational energy might be the result of interactions with lattice phonons [23, 24]. Especially, he suggested this mechanism in protein α-helix which is composed of three channels of one-dimensional spring chain coupled with each other.

Motivated by these considerations, in the present work we aim to investigate the quantum state transfer in a bio-inspired network of qubits. In particular, we consider an α-helix structure. The latter looks like a two-dimensional spin network with the pair (n, α) denoting the n-th molecule along a chain and α-th particular channel. In this model, the whole Hamiltonian is composed of three parts: the exciton energy operator, phonon energy operator, and exciton–phonon interaction operator. Usually, Davydov's phonon is a large acoustic polaron at low temperatures. Therefore, only the exciton part gives rise to a suitable candidate for the spin network. Given the fact that the propagation of quantum information over a network of spins is of great importance, we focus here only on the exciton part of Davydov's model. This in turn gives rise to four configurations based on the boundary conditions (open and closed) on both n and α. We illustrate in detail that only in one boundary condition analytical results for information transfer fidelity are obtainable. Anyway, we numerically show perfect state transfer also for other boundary conditions, but with closed boundaries for n and α.

The rest of the paper is organized as follows: In Sect. 2 we present the model and discuss the transfer fidelity and its properties. Section 3 is devoted to the special case of closed boundaries on both n and α, where an analytical investigation is possible. Sections 4, 5 and 6 deal with the other possible boundary conditions by numeric calculation. Finally, we draw our conclusion in Sect. 7.

2 The model

2.1 Davydov model

We consider a system with an α-helix structure, which is the most stable configuration of the polypeptide [25]. Due to the existence of three hydrogen bonds between peptide groups, the α-helix usually looks like a three-channel conformation each composed of a chain of springs coupled with each other. The Hamiltonian describing this system is usually referred to as Davydov's model. Its bare form without phonons reads [26]

$$\hat{H}_{\text{ex}} = \sum_{n=1}^{N} \sum_{\alpha=1}^{3} \left[E_0 \hat{B}_{n,\alpha}^\dagger \hat{B}_{n,\alpha} + J \left(\hat{B}_{n,\alpha}^\dagger \hat{B}_{n+1,\alpha} + \hat{B}_{n,\alpha}^\dagger \hat{B}_{n-1,\alpha} \right) \right.$$
$$\left. + L \left(\hat{B}_{n,\alpha}^\dagger \hat{B}_{n,\alpha+1} + \hat{B}_{n,\alpha}^\dagger \hat{B}_{n,\alpha-1} \right) \right], \tag{1}$$

where $\hat{B}_{n,\alpha}$ and $\hat{B}_{n,\alpha}^\dagger$ ($n = 1, \ldots, N$, $\alpha = 1, 2, 3$) are the spin-$\frac{1}{2}$ lowering and raising operators. The subscript n labels the molecule along a macromolecule, while the subscript α specifies a particular channel. Furthermore, E_0 is the energy of exciton (amide-I vibration), J is the nearest neighbor dipole–dipole coupling energy along a channel which is considered positive for an excited electron [27] and L is the near-

est neighbor dipole–dipole coupling energy between channels. Thus, the pair (n, α) chooses an individual amino acid. The first term can be omitted in the interaction picture since it amounts to a conserved quantity.

This system can be interpreted in terms of a spin network. Let us consider a simple undirected graph (that is, without loops or parallel edges) $G = (V, E)$, in which the vertices (nodes) $V(G) = \{1, \ldots, 3N\}$ are associated to the quantum spins. The edges $E(G)$ denote their allowed couplings.

The dimension $(2^{3N} \times 2^{3N})$ of the whole system's Hilbert space $\mathcal{H} \simeq (\mathbb{C}^2)^{\otimes 3N}$ makes pretty soon impracticable a numeric approach when N is increased. Nevertheless, the above-mentioned conserved quantity, $\hat{Q} = \sum_{n=1}^{N} \sum_{\alpha=1}^{3} \hat{B}_{n,\alpha}^{\dagger} \hat{B}_{n,\alpha}$, allows us to restrict our attention to the invariant single-excitation subspace $\mathcal{H}_1 = span\{|n\rangle\}_{n=1}^{N} \bigotimes \{|\alpha\rangle\}_{\alpha=1}^{3}$. Here, the vector $|n, \alpha\rangle = |0\rangle_{1,1}|0\rangle_{1,2} \ldots |1\rangle_{n,\alpha} \ldots |0\rangle_{N,3}$ indicates the presence of excitation in the n-th molecule and α-th channel. The $3N$ single-excitation states are conveniently labelled by an integer n running from 0 to $N-1$ within the three channels $\alpha = 1, 2, 3$. In this new basis, the $3N \times 3N$ Hamiltonian (1) describing the system is represented by the matrix

$$\hat{H}_{ex} = \begin{pmatrix} \mathbf{C}_0^0 & \mathbf{C}_1^0 & \mathbf{C}_2^0 & \cdots & \mathbf{C}_{N-1}^0 \\ \mathbf{C}_0^1 & \mathbf{C}_1^1 & \mathbf{C}_2^1 & \cdots & \mathbf{C}_{N-1}^1 \\ \vdots & & \ddots & \cdots & \vdots \\ \mathbf{C}_0^{N-1} & \mathbf{C}_1^{N-1} & \mathbf{C}_2^{N-1} & \cdots & \mathbf{C}_{N-1}^{N-1} \end{pmatrix}, \tag{2}$$

in which $\mathbf{C}_m^n$ (with $m, n = 0, \cdots N-1$) are 3×3 matrices which depend on the boundary conditions. In the next sections, we consider the possible boundary conditions in details.

2.2 Information transfer fidelity

The Hamiltonian (2) can be written as its spectral decomposition as follow

$$\hat{H}_{ex} = \sum_{n=0}^{N-1} \sum_{\alpha=1}^{3} \lambda_n^{\alpha} \hat{\prod}_n^{\alpha}, \tag{3}$$

in which λ_n^{α} are the eigenvalues of the Hamiltonian with their corresponding eigenvector $|W_n^{\alpha}\rangle$ so that we have $\hat{\prod}_n^{\alpha} = |W_n^{\alpha}\rangle\langle W_n^{\alpha}|$. Suppose the single excitation initially resides in the ith qubit at channel p, i.e., $|\psi(0)\rangle = |i, p\rangle$ with $i \in \{0, 1, \cdots, N-1\}$ and $p \in \{1, 2, 3\}$. Since $[\hat{Q}, \hat{H}_{ex}] = 0$, only the transitions of the form $|i, p\rangle \leftrightarrow |j, q\rangle$ are allowed. Therefore, we define the quantum transition probability from state $|i, p\rangle$ into $|j, q\rangle$ as follows

$$p_t([i, p], [j, q]) = |\langle i, p|e^{-i\hat{H}_{ex}t}|j, q\rangle|^2. \tag{4}$$

Using the spectral decomposition (3), the fidelity between the evolved input state and the desired output is written as

$$p_t([i, p], [j, q]) = \left| \sum_{n=0}^{N-1} \sum_{\alpha=1}^{3} \langle i, p | \prod_n^\alpha | j, q \rangle e^{-i\lambda_n^\alpha t} \right|^2. \tag{5}$$

An upper bound for the transition probability is derived by assuming that there exists t such that the phase factor $e^{-i\lambda_n^\alpha t}$ can be written as

$$e^{-i\lambda_n^\alpha t} = s_n^\alpha([i, p], [j, q])e^{i\phi}, , \quad \forall n = 0, \ldots, N-1, \quad \text{and} \quad \alpha = 1, 2, 3, \tag{6}$$

where either $s_n^\alpha([i, p], [j, q]) := \mathrm{Sgn}(\langle i, p | \prod_n^\alpha | j, q \rangle) \in \{-1, +1\}$ as a sign factor or $s_n^\alpha([i, p], [j, q]) = 0$ whenever $\langle i, p | \prod_n^\alpha | j, q \rangle = 0$ and ϕ is an arbitrary global phase which must be the same for all n's and α's. In this case, since the global phase ϕ can be absorbed in the absolute value in (5), the upper bound for the transition probability is obtained as follows [28]

$$p_{\max}([i, p], [j, q]) = \left(\sum_{n=0}^{N-1} \sum_{\alpha=1}^{3} |\langle i, p | \prod_n^\alpha | j, q \rangle| \right)^2. \tag{7}$$

The maximum amplitude for the transition probability $p_{\max}([i, p], [j, q])$ is 1, and this case is referred to as *Perfect State Transfer* (PST), see, e.g., [29, 30]. Furthermore, due to the exponential nature of the phase factor $e^{-i\lambda_n^\alpha t}$ there must exist a sequence of time samples t_n for which PST occurs.

According to Eq. (6), there exist eigenspaces with $s_n^\alpha([i, p], [j, q]) = 0$ which do not give any contribution in the sum (7); thus, they can be removed from the summation. We refer to them as *dark-state* subspaces. Then we can limit ourselves to the $K' \subseteq \{0, 1, \ldots, N-1\}$ of indices n for which $s_n^\alpha([i, p], [j, q]) \neq 0$. For simplicity let us use s_n^α instead of $s_n^\alpha([i, p], [j, q])$. Then we point out that for all members of set K' we have $s_n^\alpha = \pm 1$ and $\exp\left[-i\frac{\pi}{2}(s_n^\alpha - 1)\right] = \pm 1$. Therefore, we may write $s_n^\alpha = \exp\left[-i\pi\left(2k_n^\alpha + \frac{1}{2}(s_n^\alpha - 1)\right)\right]$ where $k_n^\alpha \in \mathbb{Z}$ are arbitrary integers. Using this relation and Eq. (6), we may obtain the following relation

$$\lambda_n^\alpha t = 2\pi k_n^\alpha + \frac{\pi}{2}(s_n^\alpha - 1) - \phi), \quad \forall n \in K' \text{ and } \alpha = 1, 2, 3. \tag{8}$$

In a pairwise manner with $[n, \alpha] \neq [m, \beta]$, the above attainability condition becomes

$$(\lambda_n^\alpha - \lambda_m^\beta)t = 2\pi(k_n^\alpha - k_m^\beta) + \frac{\pi}{2}(s_n^\alpha - s_m^\beta), \quad \forall n, m \in K' \text{ and } \alpha, \beta = 1, 2, 3, \tag{9}$$

which is more useful as it is independent of the arbitrary phase ϕ. In the above relation $k_n^\alpha, k_m^\beta \in \mathbb{Z}$ are arbitrary integers. Noting s_n^α and $s_m^\alpha = \pm 1$, we can write the attainability constraint (9) as
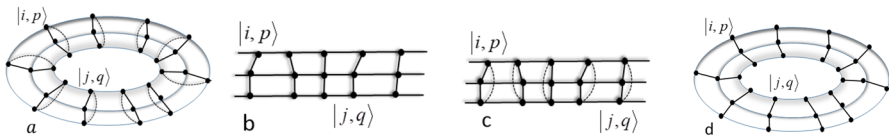
Fig. 1 The boundary conditions: **a** Closed on both N and α, **b** open on both N and α, **c** open on N and closed on α, and **d** closed on N and open on α

$$
\begin{aligned}
(\lambda_n^\alpha - \lambda_m^\beta)t &= 2\pi(k_n^\alpha - k_m^\beta), & &\text{if } s_n^\alpha = s_m^\beta, \\
(\lambda_n^\alpha - \lambda_m^\beta)t &= 2\pi(k_n^\alpha - k_m^\beta) + \pi, & &\text{if } s_n^\alpha = -s_m^\beta = 1, \\
(\lambda_n^\alpha - \lambda_m^\beta)t &= 2\pi(k_n^\alpha - k_m^\beta) - \pi, & &\text{if } s_n^\alpha = -s_m^\beta = -1.
\end{aligned} \tag{10}
$$

Note that from above equations, we look for PST between the particular input and output states ($[i, p], [j, q]$) (through the values of s_n^α and s_m^β), while the pair ($[n, \alpha], [m, \beta]$) indicates two arbitrary nodes in the network (according to the summation in Eq. (5)). The equations (10) imply that if (9) holds for the couples ($[n, \alpha], [m, \beta]$) and ($[m, \beta], [r, \eta]$), then (9) holds also for ($[n, \alpha], [r, \eta]$), with $r \in K'$ and $\alpha, \beta, \eta = 1, 2, 3$. Furthermore, the set of equations are redundant, thus, in order to consider just linear independent equations, we restrict ourselves to an appropriate subset of equations (10) with ($[n, \alpha], [n, \beta]$) where $\alpha \neq \beta$ and ($[n, \alpha], [n + 1, \beta]$) for $n \in K'$ and $\alpha, \beta = 1, 2, 3$. Moreover, note that the conditions (10) are sufficient but not necessary for PST because they guarantee the attainability of the upper bound p_{max} in (7), but it is not guaranteed that this is equal to 1 (i.e., that it gives PST).

We are in the position to apply the above-described tools, for studying the information transmission in different configurations of the spin network, determined by the possible boundary conditions. Figure 1 illustrates the topologies of the different cases investigated. The case of closed boundary conditions either along the chain and the channels is sketched in Fig. 1a, the configuration with open boundary conditions along the chain and the channels is illustrated in Fig. 1b, and the case of open (closed) boundary conditions along the chain and closed (open) conditions for the channels is described in Fig. 1c (Fig. 1d).

3 Closed boundary on both N and α

In this section, we consider the case of closed boundary conditions on both n and α (see Fig. 1a). Restricted to the single excitation subspace, the Hamiltonian of the system becomes a block circulant matrix with circulant blocks (which are also symmetric blocks). In fact, $\hat{H}_{ex}$ is a $3N \times 3N$ block circulant matrix with 3×3 circulant matrices $\mathbf{C}_0^0, \mathbf{C}_1^0, \ldots, \mathbf{C}_{N-1}^0$, where

$$
\mathbf{C}_0^0 = \begin{pmatrix} 0 & L & L \\ L & 0 & L \\ L & L & 0 \end{pmatrix}; \quad \mathbf{C}_1^0 = \mathbf{C}_{N-1}^0 = \begin{pmatrix} J & 0 & 0 \\ 0 & J & 0 \\ 0 & 0 & J \end{pmatrix} \tag{11}
$$

and $\mathbf{C}_2^0 = \mathbf{C}_3^0 = \cdots = \mathbf{C}_{N-2}^0 = 0$. Then the Hamiltonian $\hat{H}_{\text{ex}}$ has the matrix form

$$
\hat{H}_{\text{ex}} = \begin{pmatrix}
\mathbf{C}_0^0 & \mathbf{C}_1^0 & 0 & \cdots & \mathbf{C}_{N-1}^0 \\
\mathbf{C}_{N-1}^0 & \mathbf{C}_0^0 & \mathbf{C}_1^0 & & 0 \\
0 & \mathbf{C}_{N-1}^0 & \ddots & \ddots & \vdots \\
\vdots & & \ddots & & \mathbf{C}_1^0 \\
\mathbf{C}_1^0 & 0 & \cdots & \mathbf{C}_{N-1}^0 & \mathbf{C}_0^0
\end{pmatrix}.
\tag{12}
$$

The eigenvalues of $\hat{H}_{\text{ex}}$ are [31]

$$
\lambda_n^\alpha = 2J \cos\left(\frac{2\pi n}{N}\right) - 2e^{i\alpha\pi} L \cos\left(\frac{\pi}{3}(\alpha - 1)\right),
\tag{13}
$$

in which λ_n^α is the αth diagonal element of the nth 3×3 block for $n = 0, 1, 2, \ldots, N-1$ and $\alpha = 1, 2, 3$. Moreover, the normalized eigenvectors of $\hat{H}_{\text{ex}}$ are found to be [31]

$$
W_n^\alpha = \frac{1}{\sqrt{3N}} \left(\rho_n^{-1} V_\alpha, V_\alpha, \rho_n V_\alpha, \rho_n^2 V_\alpha, \ldots, \rho_n^{N-2} V_\alpha \right)^T
\tag{14}
$$

where $\rho_n = e^{i2\pi n/N}$ is the N-th Root of Unity for $n = 0, 1, \ldots, N-1$ and V_α is defined as

$$
V_1 = \left(1, 1, 1\right)^T, \quad V_2 = \left(e^{-\frac{2i\pi}{3}}, 1, e^{\frac{2i\pi}{3}}\right)^T, \quad V_3 = \left(e^{\frac{2i\pi}{3}}, 1, e^{-\frac{2i\pi}{3}}\right)^T.
\tag{15}
$$

3.1 Eigendecomposition of the Hamiltonian

We first point out that according to (13), the eigenvalues corresponding to $\alpha = 2$ and $\alpha = 3$ are equal, i.e., $\lambda_n^2 = \lambda_n^3$. This allows us to discuss the problem with the eigendecompositotion of the Hamiltonian for only two cases corresponding to $\alpha = 1$ and $\alpha = 2$ (or 3).

We begin by considering the case $\alpha = 1$:

- If N is even, but not divisible by 4, we have $\lambda_n^1 = \lambda_{N-n}^1 = -\lambda_{N/2-n}^1 = -\lambda_{N/2+n}^1 \neq 0$, which means there are $\frac{N}{2} - 1$ distinct pairs of double eigenvalues and two single eigenvalues $\pm 2J + 2L$ for $n = 0$ and $n = \frac{N}{2}$ giving totally $\tilde{N} = \frac{N}{2} + 1$ pairwise distinct eigenvalues:

$$
\left\{ -2J + 2L, \lambda_n^1, 2J + 2L : n = 1, 2, \ldots, \frac{N}{2} - 1 \right\}.
\tag{16}
$$

In this case, if N is divisible by 4, there is also a double eigenvalues at 0 for $n = \frac{N}{4}$ and $\frac{3N}{4}$ giving totally $\tilde{N} = \frac{N}{2} + 2$ pairwise distinct eigenvalues.

- If N is odd, $\lambda_n^1 = \lambda_{N-n}^1 \neq 0$ and there are $(N-1)/2$ distinct pairs of double eigenvalues and a single eigenvalue $2J + 2L$ at $n = 0$ which is totally $\tilde{N} = (N+1)/2$ distinct eigenvalues:

$$\left\{ \lambda_n^1, 2J + 2L : n = 1, 2, \ldots, \frac{N-1}{2} \right\}. \tag{17}$$

On the other hand, considering the cases $\alpha = 2$ (or $\alpha = 3$), we have:

- If N is even, but not divisible by 4, we have $\lambda_n^\alpha = \lambda_{N-n}^\alpha = -\lambda_{N/2-n}^\alpha = -\lambda_{N/2+n}^\alpha \neq 0$ and so $\frac{N}{2} - 1$ distinct pairs of the double eigenvalues and two single eigenvalues $\pm 2J - L$ giving totally $\tilde{N} = \frac{N}{2} + 1$ pairwise distinct eigenvalues:

$$\left\{ -2J - L, \lambda_n^\alpha, 2J - L : \alpha = 2 \quad (\text{or} \quad 3) \quad \text{and} \quad n = 1, 2, \ldots, \frac{N}{2} - 1 \right\}. \tag{18}$$

If N is divisible by 4, a double eigenvalue at 0 for $n = \frac{N}{4}$ and $\frac{3N}{4}$ giving totally $\tilde{N} = \frac{N}{2} + 2$ pairwise distinct eigenvalues.
- If N is odd, $\lambda_n^\alpha = \lambda_{N-n}^\alpha \neq 0$, we have $(N-1)/2$ distinct pairs of double eigenvalues and a single eigenvalue $2J - L$ at $n = 0$ which is totally $\tilde{N} = (N+1)/2$ distinct eigenvalues:

$$\left\{ \lambda_n^\alpha, 2J - L : \alpha = 2 \quad (\text{or} \quad 3) \quad \text{and} \quad n = 1, 2, \ldots, \frac{N-1}{2} \right\} \tag{19}$$

Now we are in a position to construct the eigendecomposition of the Hamiltonian. To this end, we first define for the both even and odd N, the eigenprojection on the corresponding double eigenvalue $\lambda_n^\alpha = \lambda_{N-n}^\alpha$ to be as $\prod_n^\alpha := |W_n^\alpha\rangle\langle W_n^\alpha| + |W_{N-n}^\alpha\rangle\langle W_{N-n}^\alpha|$. Also, we consider the eigenprojection of the eigenvalue at $n = 0$ as $\prod_0^\alpha := |W_0^\alpha\rangle\langle W_0^\alpha|$. Finally, if N is even, the eigenprojection of the eigenvalue at $n = N/2$ is $\prod_{N/2}^\alpha := |W_{N/2}^\alpha\rangle\langle W_{N/2}^\alpha|$ and further, if N is divisible by 4, then we define also $\prod_{N/4}^\alpha := |W_{N/4}^\alpha\rangle\langle W_{N/4}^\alpha| + |W_{3N/4}^\alpha\rangle\langle W_{3N/4}^\alpha|$ for the corresponding eigenvalues at $n = N/4$ and $n = 3N/4$. With this notation, the spectral decomposition (3) for the Hamiltonian (12) will be

$$\hat{H}_{\text{ex}} = \sum_{n=0}^{\tilde{N}-1} \sum_{\alpha=1}^{3} \lambda_n^\alpha \prod_n^\alpha. \tag{20}$$

Then as mentioned above in Sect. (2.2), to avoid having redundant equations of (10) we limit ourselves only to the linear independent equations for $([n, 1], [n, 2])$ where $n \in K' = \{0, 1, \ldots, \tilde{N}-1\}$ and $([n, \alpha], [n+1, \beta])$ where $n \in K' = \{0, 1, \ldots, \tilde{N}-2\}$ and $\alpha, \beta = 1, 2$ (or 3).

3.2 Dark states

In order to find the dark states of our $3N$-qubit system, we should study when $s_n^\alpha([i, p], [j, q]) = 0$. According to the Sect. 3.1, we point out that for $n = 0$, we have

$$
\begin{aligned}
\langle i, p|\Pi_0^1|j, q\rangle &= 1/3N \neq 0, \\
\langle i, p|\Pi_0^2|j, q\rangle &= e^{2\mathrm{i}(p-q)\pi/3}/3N \neq 0, \\
\langle i, p|\Pi_0^3|j, q\rangle &= e^{2\mathrm{i}(q-p)\pi/3}/3N \neq 0.
\end{aligned}
\tag{21}
$$

This means there is no dark state with respect to $n = 0$ (with multiplicity of 1) for any value of α. Also, for an even N, there is the eigenvalue with multiplicity of 1 with respect to $n = N/2$. It is straightforward to illustrate the following relation for the case $n = N/2$:

$$
\begin{aligned}
\langle i, p|\Pi_{N/2}^1|j, q\rangle &= (-1)^{(i-j)}/3N \neq 0, \\
\langle i, p|\Pi_{N/2}^2|j, q\rangle &= (-1)^{(i-j)}e^{2\mathrm{i}(p-q)\pi/3}/3N \neq 0, \\
\langle i, p|\Pi_{N/2}^3|j, q\rangle &= (-1)^{(i-j)}e^{2\mathrm{i}(q-p)\pi/3}/3N \neq 0.
\end{aligned}
\tag{22}
$$

Therefore, there is no dark state associated with $n = N/2$ for an even N. Furthermore, for the eigenvalues with multiplicity 2 (i.e., $\lambda_n^\alpha = \lambda_{N-n}^\alpha$ with $\alpha = 1, 2, 3$) we have

$$
\begin{aligned}
\langle i, p|\Pi_n^1 + \Pi_{N-n}^1|j, q\rangle &= 2\cos\left(2\pi n(j-i)/N\right)/3N, \\
\langle i, p|\Pi_n^2 + \Pi_{N-n}^2|j, q\rangle &= 2\cos\left(2\pi n(j-i)/N\right)e^{2\mathrm{i}(p-q)\pi/3}/3N, \\
\langle i, p|\Pi_n^3 + \Pi_{N-n}^3|j, q\rangle &= 2\cos\left(2\pi n(j-i)/N\right)e^{2\mathrm{i}(q-p)\pi/3}/3N,
\end{aligned}
\tag{23}
$$

for $n = 1, \ldots, \lceil(N - 3)/2\rceil$. According to the relations (23), it is obvious that for all values of α, there are dark states if $\cos\left(2\pi n(j - i)/N\right) = 0$, i.e., when $4n(j - i)/N$ is an odd integer. Thus, we can say that the divisibility of N by 4 is a necessary but not sufficient condition to have dark states due to the term $(j - i)$ relevant to the input and output states.

Our calculations show that $p_{max}([i, p], [j, q])$ in (7) is always 1 (independent on input and output qubits) due to the fact that the analytical eigenvectors of the Hamiltonian (12) are the Kronecker product of two Fourier matrices (14) where each element of the eigenvectors has the same structure as $e^{\mathrm{i}\phi}/\sqrt{3N}$.

In what follows we use the rescaled time $\tau = Lt$ and the dimensionless parameter $\gamma = J/L$ in our all analytical and numerical computations.

Example: Now we aim to analytically explore the attainability conditions (10) of $p_\tau([i, p], [j, q])$ for $N = 8$ qubits with the channels $\alpha = 1, 2$ and 3. According to Sect. 3.1, there are 6 pairwise distinct eigenvalues, i.e., $\tilde{N} = 6$. Choosing the suitable subset $\mathcal{S} \subseteq K' \times K'$ where $K' = \{0, 1, \ldots, 5\}$, the attainability condition (9) becomes

$$
(\lambda_n^\alpha - \lambda_m^\beta)\tau = \tau\left(-4\gamma \sin(\frac{\pi}{N}(n + m))\sin(\frac{\pi}{N}(n - m))\right)
$$

$$-2\left(e^{i\alpha\pi}\cos\left(\frac{\pi}{3}(\alpha-1)\right)-e^{i\beta\pi}\cos\left(\frac{\pi}{3}(\beta-1)\right)\right);$$
$$\forall n, m \in K' = \{0, 1, \ldots, 5\}; \text{ and } \alpha, \beta \in \{1, 2\}. \tag{24}$$

Now in order to have linear independent equations, we consider several specific cases:

- We first restrict ourselves to the subset $([n, \alpha], [n+1, \beta])$ where $n \in K' = \{0, 1, \ldots, \tilde{N}-2\}$ and $\alpha = \beta \in \{1, 2\}$. From (24) we obtain

$$(\lambda_n^\alpha - \lambda_{n+1}^\alpha)\tau = -4\gamma \sin\left(\frac{\pi}{N}(2n+1)\right)\sin\left(\frac{\pi}{N}\right)\tau,$$
$$\forall n \in K' = \{0, 1, 2, 3, 4\}; \text{ and } \alpha \in \{1, 2\}. \tag{25}$$

Then from the attainability condition (10), we derive

$$\begin{aligned}
(\lambda_0^\alpha - \lambda_1^\alpha)\tau &= (2-\sqrt{2})\gamma\tau = 2\pi(k_0^\alpha - k_1^\alpha), & s_0^\alpha &= s_1^\alpha, \\
(\lambda_0^\alpha - \lambda_1^\alpha)\tau &= (2-\sqrt{2})\gamma\tau = 2\pi(k_0^\alpha - k_1^\alpha) + \pi, & s_0^\alpha &= -s_1^\alpha = 1, \\
(\lambda_0^\alpha - \lambda_1^\alpha)\tau &= (2-\sqrt{2})\gamma\tau = 2\pi(k_0^\alpha - k_1^\alpha) - \pi, & s_0^\alpha &= -s_1^\alpha = -1,
\end{aligned} \tag{26}$$

and also

$$\begin{aligned}
(\lambda_1^\alpha - \lambda_2^\alpha)\tau &= \sqrt{2}\gamma\tau = 2\pi(k_1^\alpha - k_2^\alpha), & s_1^\alpha &= s_2^\alpha, \\
(\lambda_1^\alpha - \lambda_2^\alpha)\tau &= \sqrt{2}\gamma\tau = 2\pi(k_1^\alpha - k_2^\alpha) + \pi, & s_1^\alpha &= -s_2^\alpha = 1, \\
(\lambda_1^\alpha - \lambda_2^\alpha)\tau &= \sqrt{2}\gamma\tau = 2\pi(k_1^\alpha - k_2^\alpha) - \pi, & s_1^\alpha &= -s_2^\alpha = -1,
\end{aligned} \tag{27}$$

Besides, $(\lambda_0^\alpha - \lambda_1^\alpha) = (\lambda_3^\alpha - \lambda_4^\alpha) = (\lambda_4^\alpha - \lambda_5^\alpha)$ and $(\lambda_1^\alpha - \lambda_2^\alpha) = (\lambda_2^\alpha - \lambda_3^\alpha)$.
- Secondly, we consider the restricted subset $([n, \alpha], [n+1, \beta])$ where $n \in K' = \{0, 1, \ldots, \tilde{N}-2\}$ while $\alpha \neq \beta \in \{1, 2\}$. Then, from equation (24) we have

$$\begin{aligned}
(\lambda_n^\alpha - \lambda_{n+1}^\beta)\tau = \tau\Big(&-4\gamma\sin\left(\frac{\pi}{N}(2n+1)\right)\sin\left(\frac{\pi}{N}\right) \\
&-2\left(e^{i\alpha\pi}\cos\left(\frac{\pi}{3}(\alpha-1)\right) - e^{i\beta\pi}\cos\left(\frac{\pi}{3}(\beta-1)\right)\right)\Big) \\
&\forall n \in K' = \{0, 1, 2, 3, 4\}; \text{ and } \alpha \neq \beta \in \{1, 2\}.
\end{aligned} \tag{28}$$

Then the condition (10) implies

$$\begin{aligned}
(\lambda_0^\alpha - \lambda_1^\beta)\tau &= ((2-\sqrt{2})\gamma + 3)\tau = 2\pi(k_0^\alpha - k_1^\beta), & s_0^\alpha &= s_1^\beta, \\
(\lambda_0^\alpha - \lambda_1^\beta)\tau &= ((2-\sqrt{2})\gamma + 3)\tau = 2\pi(k_0^\alpha - k_1^\beta) + \pi, & s_0^\alpha &= -s_1^\beta = 1, \\
(\lambda_0^\alpha - \lambda_1^\beta)\tau &= ((2-\sqrt{2})\gamma + 3)\tau = 2\pi(k_0^\alpha - k_1^\beta) - \pi, & s_0^\alpha &= -s_1^\beta = -1,
\end{aligned} \tag{29}$$

and also

$$
\begin{aligned}
(\lambda_1^\alpha - \lambda_2^\beta)\tau &= (\sqrt{2}\gamma + 3)\tau = 2\pi(k_1^\alpha - k_2^\beta), & s_1^\alpha &= s_2^\beta, \\
(\lambda_1^\alpha - \lambda_2^\beta)\tau &= (\sqrt{2}\gamma + 3)\tau = 2\pi(k_1^\alpha - k_2^\beta) + \pi, & s_1^\alpha &= -s_2^\beta = 1, \\
(\lambda_1^\alpha - \lambda_2^\beta)\tau &= (\sqrt{2}\gamma + 3)\tau = 2\pi(k_1^\alpha - k_2^\beta) - \pi, & s_1^\alpha &= -s_2^\beta = -1.
\end{aligned} \tag{30}
$$

Moreover, $(\lambda_0^\alpha - \lambda_1^\beta) = (\lambda_3^\alpha - \lambda_4^\beta) = (\lambda_4^\alpha - \lambda_5^\beta)$ and $(\lambda_1^\alpha - \lambda_2^\beta) = (\lambda_2^\alpha - \lambda_3^\beta)$.

- Finally, we choose the subset $([n, \alpha], [n, \alpha+1])$ where $n \in K' = \{0, 1, \ldots, \tilde{N}-1\}$ and $\alpha = 1$ to find other linear independent equations of (24) given by

$$
(\lambda_n^\alpha - \lambda_n^{\alpha+1})\tau = -2\tau \left(e^{i\alpha\pi} \cos\left(\frac{\pi}{3}(\alpha - 1)\right) - e^{i\beta\pi} \cos\left(\frac{\pi}{3}(\alpha)\right) \right),
$$
$$
\forall n \in K' = \{0, 1, \ldots, 5\}; \text{ and } \alpha = 1. \tag{31}
$$

Based on this choice, from the attainability condition (10) we obtain

$$
\begin{aligned}
(\lambda_n^1 - \lambda_n^2)\tau &= 3\tau = 2\pi(k_n^1 - k_n^2), & s_n^1 &= s_n^2, \\
(\lambda_n^1 - \lambda_n^2)\tau &= 3\tau = 2\pi(k_n^1 - k_n^2) + \pi, & s_n^1 &= -s_n^2 = 1, \\
(\lambda_n^1 - \lambda_n^2)\tau &= 3\tau = 2\pi(k_n^1 - k_n^2) - \pi, & s_n^1 &= -s_n^2 = -1.
\end{aligned} \tag{32}
$$

Summarizing, given that there are solutions to Eq. (10) for the above three cases, we could attain PST. However, our numerical investigations indicate only PST happens when the in and out nodes are in the same channel diametrically opposed. This confirms that the analytical solutions are necessary but not sufficient conditions to have PST which to pointed already in Sect. 2.2. In other words, in this example we should only deal with Eq. (25) in order to look for the equivalence between the analytical solutions with the numerical dynamics of the transmission probability as a function of τ and γ. Figure 2a illustrates the transmission probability p_τ versus τ when $N = 8$ and for two different values of γ, between two diametrically opposed nodes in the same channel as $p_\tau([0, 1], [4, 1])$. It is evident the possibility of PST for both $\gamma = 3$ and $\gamma = 5$. The analytical attainability $p_\tau([i, p], [j, q])$ for the condition (27) as $\sqrt{2}\gamma\tau = 2\pi(k_1^\alpha - k_2^\alpha) - \pi$ with $\gamma = 3$, $\tau = 12.59, 73.31, 134.03, \cdots$ and $k_1^\alpha - k_2^\alpha = 8, 49, 90, \cdots$ shows the consistency with the numerical outcome $p_\tau([0, 1], [4, 1]) = 1$. The same agreement between analytical and numerical solutions of $p_\tau([0, 1], [4, 1]) = 1$ is also seen for $\gamma = 5$ where $\tau = 43.985, 131.955 \cdots$ for $k_1^\alpha - k_2^\alpha = 49, 148, \cdots$. More generally, we display the minimum values τ_{min} at which the probability $p_\tau([0, 1], [4, 1]) = 1$ versus γ for $N = 8$ in Fig. 2b. Values of τ_{min} saturating the range of the figure mean that the probability never reaches 1. Then for $\gamma \to \infty$, i.e., $L \to 0$, finite values of t_{min} become more frequent depicted in Fig. 2c. Thus, this can be understood with the fact that in such a limiting case the information is not spread over three channels, but remains confined within only one channel.
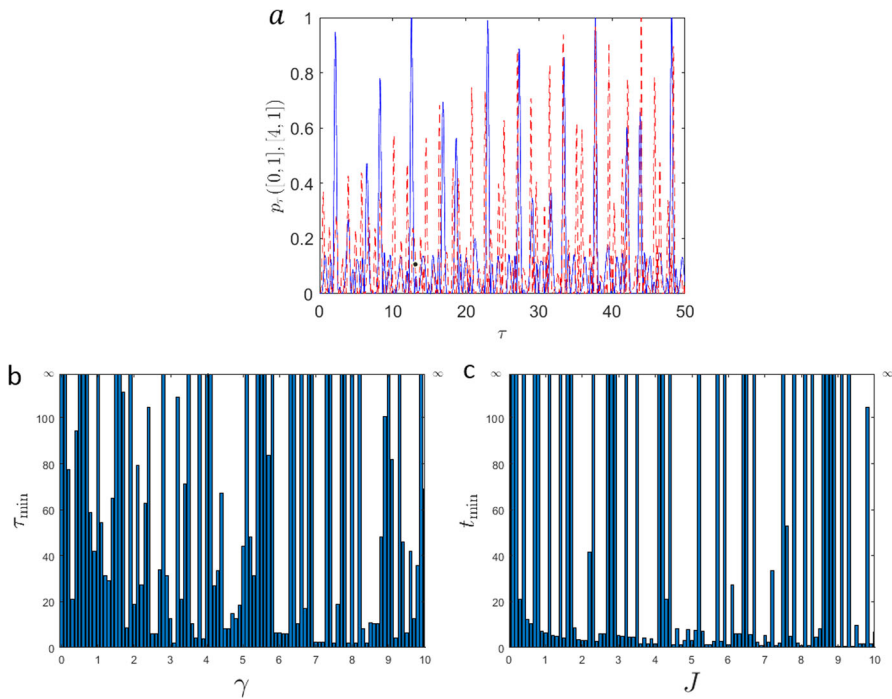
Fig. 2 The transmission probability $p_\tau([0, 1], [4, 1])$ of a spin network with $N = 8$ nodes and closed boundary on both N and α; **a** p_τ versus τ for $\gamma = 3$ (solid blue line) and $\gamma = 5$ (red dashed line), **b** the minimum value τ_{min} versus γ at which $p_\tau = 1$ for the finite values of γ, and **c** the minimum value t_{min} versus J at which $p_t = 1$ for $\gamma \to \infty$, i.e., $L \to 0$

4 Open boundary on both N and α

The second condition we consider is the open boundary on both N and α (see Fig. 1b). In such a case, the Hamiltonian belongs to the symmetric block-Toeplitz tridiagonal matrices which can be displayed as

$$\hat{H}_{ex} = \begin{pmatrix} \mathbf{C}_0^0 & \mathbf{C}_1^0 & 0 & \cdots & 0 \\ \mathbf{C}_0^1 & \mathbf{C}_0^0 & \mathbf{C}_1^0 & & 0 \\ 0 & \mathbf{C}_0^1 & \ddots & \ddots & \vdots \\ \vdots & & \ddots & & \mathbf{C}_1^0 \\ 0 & 0 & \cdots & \mathbf{C}_0^1 & \mathbf{C}_0^0 \end{pmatrix}$$

with

$$\mathbf{C}_0^0 = \begin{pmatrix} 0 & L & 0 \\ L & 0 & L \\ 0 & L & 0 \end{pmatrix}; \qquad \mathbf{C}_0^1 = \mathbf{C}_1^0 = \begin{pmatrix} J & 0 & 0 \\ 0 & J & 0 \\ 0 & 0 & J \end{pmatrix}. \tag{33}$$
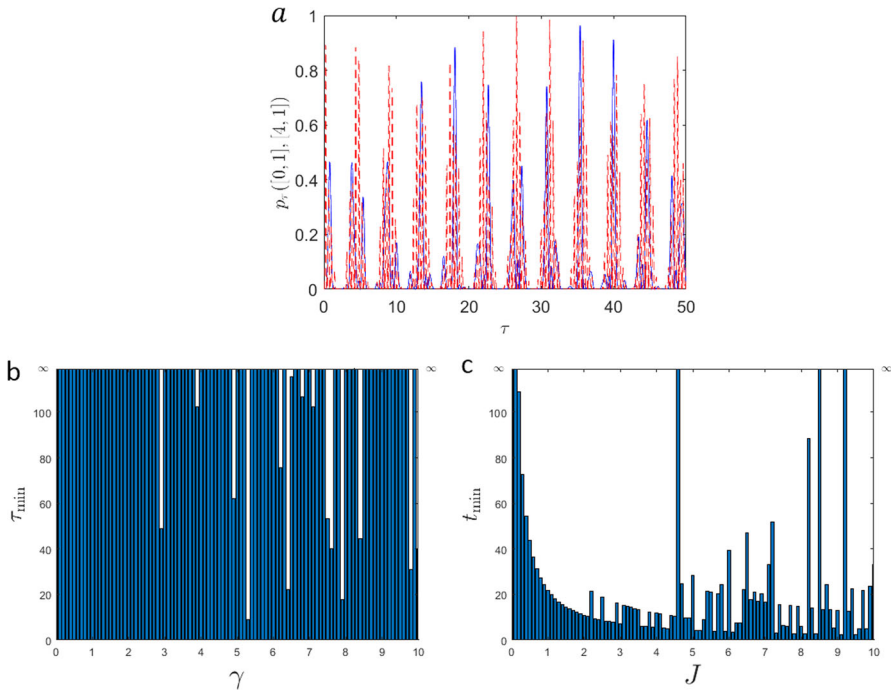
Fig. 3 The transmission probability $p_\tau([0, 1], [4, 1])$ of a spin network with $N = 5$ nodes and open boundary on both N and α; **a** p_τ versus τ for $\gamma = 4$ (solid blue line) and $\gamma = 15$ (red dashed line), **b** the minimum value τ_{min} versus γ at which $p_\tau = 1$ for the finite values of γ, and **c** the minimum value t_{min} versus J at which $p_t = 1$ for $\gamma \to \infty$, i.e., $L \to 0$

The eigenvalues of the above matrix $\hat{H}_{ex}$ are [32]

$$\lambda_n^\alpha = 2J \cos((n + 1)\pi/N + 1) + 2L \cos(\alpha\pi/4), \tag{34}$$

where $\alpha = 1, 2, 3$ and $n = 0, 1, \ldots, N - 1$.

Given the fact that in this case, it is impossible to analytically find the eigenvectors of the Hamiltonian, we are obligated to numerically study the transmission probability p_τ in (5). Note that only $p_\tau([0, 1], [4, 1])$ and $p_\tau([0, 1], [4, 3])$ enjoy PST and we choose to show $p_\tau([0, 1], [4, 1])$ to have coherency with other boundary conditions. Figure 3 shows the probability of the state transmission in the same channel $p_\tau([0, 1], [4, 1])$ with the number of sites $N = 5$. We see from Fig. 3a the behavior of p_τ versus τ where PST is observable for $\gamma = 15$ when $\tau = 26.6, 84.4, \cdots$, however there is no PST for $\gamma = 4$. Figure 3b displays the smallest time τ_{min} at which PST is achieved versus the finite values of γ. As can be seen, finite τ_{min} are quite rare, meaning that PST does not occur for most of the γ values. Figure 3c shows that for $L \to 0$ most of the values of τ_{min} become finite and actually they generically tend to decrease with J.

5 Open boundary on *N* and closed boundary on *α*

The third condition is the open boundary on N and closed boundary on α (see Fig. 1c) which again is a block-Toeplitz tridiagonal matrix as in (4); however, here

$$\mathbf{C}_0^0 = \begin{pmatrix} 0 & L & L \\ L & 0 & L \\ L & L & 0 \end{pmatrix} \qquad (35)$$

and $\mathbf{C}_0^1 = \mathbf{C}_1^0 = J I_{3\times 3}$.. Then the eigenvalues will be [32]

$$\lambda_n^\alpha = 2J \cos\left((n+1)\pi/N+1\right) + 2L \cos\left(2\pi\alpha/3\right), \qquad (36)$$

where $\alpha = 1, 2, 3$, and $n = 0, 1, \ldots, N-1$. Our investigations show that PST can be only reachable between the nodes with the longest distance in the same channel for specific γ. Figure 4 shows the transmission probability $p_\tau[(0, 1), (3, 1)]$ with $N = 4$. PST can be seen in Fig. 4a for $\gamma = 9.4$ when $\tau = 8.35, 39.75, 56.5, \cdots$, while it does not occur for $\gamma = 4$. Figure 4b shows the least amounts of time to wait for PST versus finite values of γ. It is observed that PST does not occur for several values of γ. However, Fig. 4c is an evidence of well spreading of information over only one channel due to the finiteness and decreasing behavior of t_{min} versus J when $L \to 0$, i.e., $\gamma \to \infty$.

6 Closed boundary on *N* and open boundary on *α*

The last boundary condition to be considered is closed on N and open on α (see Fig. 1d). This gives rise to a $3N \times 3N$ block circulant matrix in the form (12) with 3×3 symmetric blocks

$$\mathbf{C}_0^0 = \begin{pmatrix} 0 & L & 0 \\ L & 0 & L \\ 0 & L & 0 \end{pmatrix}; \qquad \mathbf{C}_1^0 = \mathbf{C}_{N-1}^0 = \begin{pmatrix} J & 0 & 0 \\ 0 & J & 0 \\ 0 & 0 & J \end{pmatrix} \qquad (37)$$

and $\mathbf{C}_2^0 = \mathbf{C}_3^0 = \cdots = \mathbf{C}_{N-2}^0 = 0$. Our numerical investigations show no attainability for finite values of γ between any in and out nodes. The highest transmission probability (around 0.8) is achievable between diametrically opposed nodes in the same channel. In Fig. 5, we report $p_\tau[(0, 1), (3, 1)]$ for a network with $N = 6$. Fig. 5a shows p_τ versus τ for two different values of γ, and Fig. 5b displays the minimum time to wait for PST versus the coupling constant J. It can be seen that PST is rare even when $\gamma \to \infty$, i.e., $L \to 0$. Comparing these outcomes with the ones of Sect. 3, we realize a remarkable effect of boundary on α (when it is closed, PST is much more frequent).
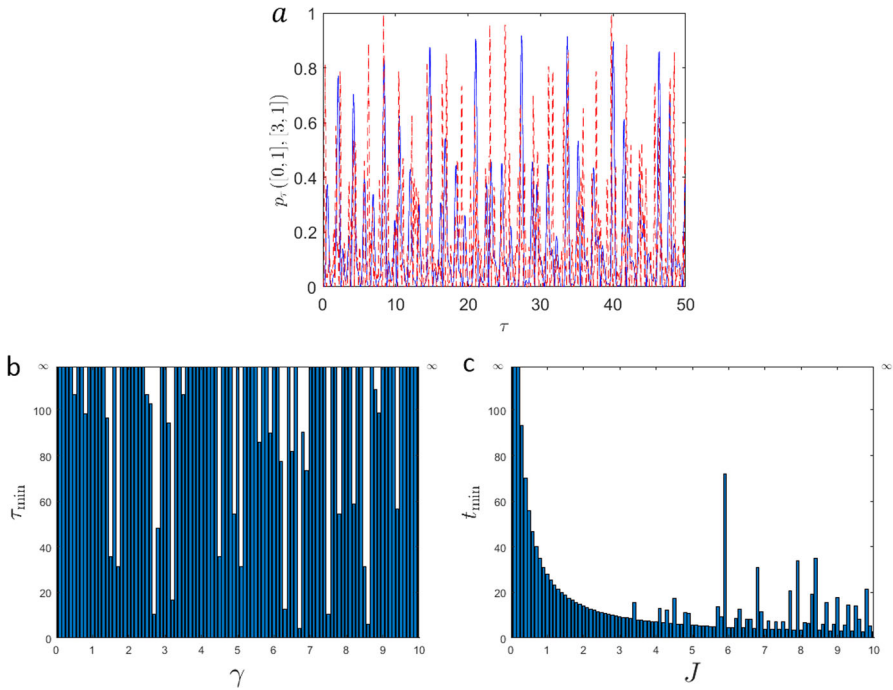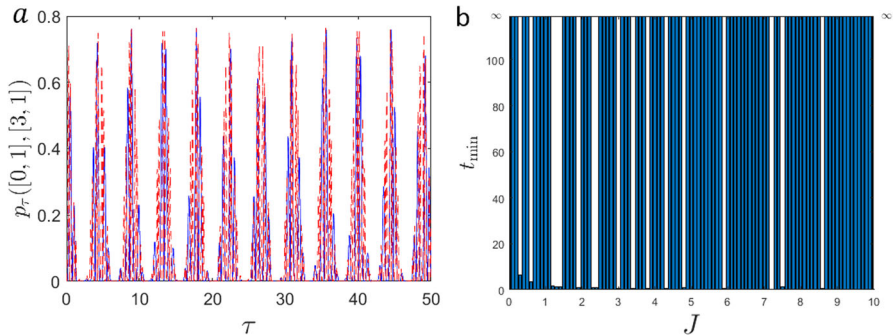
Fig. 4 The transmission probability $p_\tau([0, 1], [3, 1])$ of a spin network with $N = 4$ nodes and open boundary on N and closed boundary on α; **a** p_τ versus τ for $\gamma = 4$ (solid blue line) and $\gamma = 9.4$ (red dashed line), **b** the minimum value τ_{min} versus γ at which $p_\tau = 1$ for the finite values of γ, and **c** the minimum value t_{min} versus J at which $p_t = 1$ for $\gamma \to \infty$, i.e., $L \to 0$

Fig. 5 The transmission probability $p_\tau([0, 1], [3, 1])$ of a spin network with $N = 6$ nodes and closed boundary on N and open boundary on α; **a** p_τ versus τ for $\gamma = 4$ (solid blue line) and $\gamma = 8.25$ (red dashed line), **b** the minimum value t_{min} versus J at which $p_t = 1$ for $\gamma \to \infty$, i.e., $L \to 0$

7 Conclusions

We have studied information transfer fidelity and PST between nodes in a bio-inspired spin network of an α-helix structure of a protein using the Davydov Hamiltonian without the phononic environment by assuming the single excitation subspace. We have worked out the quantum state transmission probability for four different cyclic and non-cyclic boundary conditions on both sites and channels of the α-helix network. For only one of the boundaries, it was possible to find the analytical eigenvectors of the Hamiltonian and thus investigate the analytical scale times where PST happens. Numerical computations are in compliance with them. We reported numerically the transmission probability and the possibility of PST for other boundaries which are influenced strongly by the coupling terms in the Hamiltonian because PST needs the coupling parameters to provide the right phase matching, admitting the perfect transfer of both amplitude and phase of a quantum state from one node to another. In so doing, the analytical solutions are found to be sufficient but not necessary conditions with respect to the closed boundary on both the sites N and the channels α. In such a case, PST happens frequently during the time when the nodes are only diametrically opposed in the same channel; but considering only one or two of the boundaries open leads to the PST over fewer times, i.e., open boundary on both N and α, and open boundary on N and closed boundary on α. Finally, no attainability is observed for the case of closed boundary on N and open boundary on α; nevertheless, the highest transmission probability happens for the diametrical opposition of the input and out nodes in the same channel. Further developments of this model could take into account the effects of local or quasi-local environments [33]. Looking ahead not only quantum information transmission, but also quantum information processing could be investigated in a model involving electrons distribution [34].

Finally, we should notice that the present study was inspired by a biological system that could be implemented experimentally with a molecular spin network created by spin-labeling peptides in a synthetic polyproline (protein secondary structure) coated on a diamond membrane [35]. In such a scheme, the qubit-qubit interaction is possible as experimentally reported and evidently seen by diluting the under-investigated labeled peptides with only a few unlabeled ones in the spin network. It is notable that the electron qubits are well localized because of the hard backbone of the polyproline resisting decoherency of the phonon environment, even in low temperatures.

Data availability All relevant data have been included in the paper.

Declarations

Conflict of interest The authors declare that they have no conflict of interest.

References

1. Caruso, F., Giovannetti, V., Lupo, C., Mancini, S.: Quantum channels and memory effects. Rev. Mod. Phys. **86**, 1203 (2014)
2. Yoshida, B., Yao, N.Y.: Disentangling scrambling and decoherence via quantum teleportation. Phys. Rev. X **9**, 011006 (2019)
3. Valivarthi, R., et al.: Teleportation systems toward a quantum internet. PRX Quantum **1**, 020317 (2020)
4. Gisin, N., Thew, R.: Quantum communication. Nat. Photon. **1**, 165 (2007)
5. Ladd, T.D., et al.: Quantum computers. Nature **464**, 45 (2010)
6. Pirandola, S., et al.: Advances in quantum teleportation. Nat. Photon. **9**, 641 (2015)
7. Hou, P.-Y., et al.: Quantum teleportation from light beams to vibrational states of a macroscopic diamond. Nat. Commun. **7**, 11736 (2016)
8. Lloyd, S., et al.: Closed timelike curves via postselection: theory and experimental test of consistency. Phys. Rev. Lett. **106**, 040403 (2011)
9. Bose, S.: Quantum communication through an unmodulated spin chain. Phys. Rev. Lett. **91**, 207901 (2003)
10. Jafarizadeh, M.A., Sufiani, R.: Perfect state transfer over distance-regular spin networks. Phys. Rev. A **77**, 022315 (2008)
11. Casaccino, A., Lloyd, S., Mancini, S., Severini, S.: Quantum state transfer through a qubit network with energy shifts and fluctuations. Int. J. Quantum Inf. **07**, 1417 (2009)
12. Vafafard, A., Nourmandipour, A., Franzosi, R.: Multipartite stationary entanglement generation in the presence of dipole-dipole interaction in an optical cavity. Phys. Rev. A **105**, 052439 (2022)
13. Marais, A., et al.: The future of quantum biology. Interface **15**, 20180640 (2018)
14. Fisher, M.P.: Quantum cognition: the possibility of processing with nuclear spins in the brain. Ann. Phys. **362**, 593 (2015)
15. Engel, G.S.: Quantum coherence in photosynthesis. Procedia Chem. **3**, 222 (2011)
16. Ritz, T., et al.: Resonance effects indicate a radical-pair mechanism for avian magnetic compass. Nature **429**, 177 (2004)
17. Olaya-Castro, A., Nazir, A., Fleming, G.R.: Quantum-coherent energy transfer: implications for biology and new energy technologies. Philos. Trans. A Math. Phys. Eng. Sci. **370**, 3613 (2012)
18. Mohseni, M., Rebentrost, P., Lloyd, S., Aspuru-Guzik, A.: Environment-assisted quantum walks in energy transfer of photosynthetic complexes. J. Chem. Phys. **129**, 174106 (2008)
19. Caruso, F., et al.: Entanglement and entangling power of the dynamics in light-harvesting complexes. Phys. Rev. A **81**, 062346 (2010)
20. Engel, G.S., et al.: Evidence for wavelike energy transfer through quantum coherence in photosynthetic systems. Nature **446**, 782 (2007)
21. Fröhlich, H., Pelzer, H., Zienau, S.: XX. Properties of slow electrons in polar materials. Lond. Edinb. Dublin Philos. Mag. J. Sci. **41**, 221 (1950)
22. Holstein, T.: Studies of polaron motion: Part I. The molecular-crystal model. Ann. Phys. **8**, 325 (1959)
23. Davydov, A.S.: Solitons in Molecular Systems. Springer, Berlin (1985)
24. Scott, A.: Davydov's soliton. Phys. Rep. **217**, 1 (1992)
25. Errington, N., Iqbalsyah, T., Doig, A.J.: Structure and stability of the α-Helix: lessons for design. In: Protein Design: Methods and Applications. Humana Press, Totowa (2006)
26. Davydov, A.: The theory of contraction of proteins under their excitation. J. Theor. Biol. **38**, 559 (1973)
27. Davydov, A.: The role of solitons in the energy and electron transfer in one-dimensional molecular systems. Phys. D Nonlinear Phenom. **3**, 1 (1981)
28. Jonckheere, E., Langbein, F.C., Schirmer, S.G.: Information transfer fidelity in spin networks and ring-based quantum routers. Quantum Inf. Process. **14**, 4751 (2015)
29. Franzosi, R., Vaia, R.: Newton's cradle analogue with Bose-Einstein condensates. J. Phys. B Atomic Mol. Opt. Phys. **47**, 095303 (2014)
30. Jonckheere, E., Schirmer, S.G., Langbein, F.C.: Geometry and curvature of spin networks. In: IEEE International Conference on Control Applications, pp. 786–791 (2011)
31. Tee, G.J.: Eigenvectors of block circulant and alternating circulant matrices. N. Z. J. Math. **36**, 195 (2007)
32. Abderramán Marrero, J., Aiat Hadj, D.: Improving formulas for the eigenvalues of finite block-Toeplitz tridiagonal matrices. Appl. Math. Comput. **382**, 125324 (2020)

33. Nourmandipour, A., Tavassoly, M.K., Mancini, S.: The entangiling power of a "glocal" disspative map. Quantum Inf. Comput. **16**, 969 (2016)
34. Mancini, S., Martins, A.M., Tombesi, P.: Quantum logic with a single trapped electron. Phys. Rev. A **61**, 012303 (1999)
35. Schlipf, L., et al.: A molecular quantum spin network controlled by a single qubit. Sci. Adv. **3**, 1701116 (2017)